MEG abnormalities highlight mechanisms of surgical failure in neocortical epilepsy

Thomas W. Owen[1], Gabrielle M. Schroeder[1], Vytene Janiukstyte[1],
Gerard R. Hall[1], Andrew McEvoy[3], Anna Miserocchi[3], Jane de Tisi[3],
John S. Duncan[3], Fergus Rugg-Gunn[3], Yujiang Wang[1,2,3], Peter N. Taylor[1,2,3]

1. CNNP Lab (www.cnnp-lab.com), Interdisciplinary Computing and Complex BioSystems Group, School of Computing, Newcastle University, Newcastle upon Tyne, United Kingdom

2. Faculty of Medical Sciences, Newcastle University, Newcastle upon Tyne, United Kingdom

3. UCL Queen Square Institute of Neurology, Queen Square, London, United Kingdom

Correspondence may be addressed to:

t.w.owen1@newcastle.ac.uk and

peter.taylor@newcastle.ac.uk

Abstract

Neocortical epilepsy surgery fails to achieve post-operative seizure freedom in 30-40% of cases. It is not fully understood why surgical interventions in some patients are unsuccessful. Comparing interictal MEG bandpower from patient data to normative maps, which describe healthy spatial and population variability, we identify patient specific abnormalities relating to surgical failure. Here we propose three possible mechanisms that could contribute to a poor surgical outcome; 1) failure to resect the epileptogenic abnormalities (mislocalisation), 2) failing to remove *all* of the epileptogenic abnormalities (partial resection), and 3) insufficiently impacting the overall cortical abnormality. In this study we develop markers of these mechanisms, validating them against patient outcomes.

Resting-state eyes-closed MEG recordings were acquired for 70 healthy controls and 32 patients with refractory neocortical epilepsy. Relative band power spatial maps for five frequency bands were computed using source localised recordings from healthy controls. Patient and region-specific bandpower abnormalities were estimated as the maximum absolute z-score across all five frequency bands using healthy data as a baseline. Resected regions were identified using post-operative T1w MRI. We hypothesised that our mechanistically interpretable markers would discriminate patients with and without post-operative seizure freedom (ILAE 1 vs ILAE 2+).

Mechanisms of surgical failure discriminate surgical outcome groups (Abnormalities not targeted: AUC=0.80, p=0.003, Partial resection of the epileptogenic zone: AUC=0.68, p=0.053, Insufficient cortical abnormality impact: AUC=0.64, p=0.096), performing as well as commonly collected clinical demographics. Leveraging all mechanisms together found that 95% of those who were not seizure free had markers of surgical failure for at least one of the three proposed mechanisms. In contrast, of those patients without markers for any mechanism, 80% were ultimately seizure-free post-surgically.

The mapping of abnormalities across the brain is important for a wide range of neurological conditions. Here we have demonstrated that interictal MEG bandpower mapping has merit for the localisation of pathology, and improving our mechanistic understanding of epilepsy. Our mechanisms of surgical failure, in addition to others, could be used by future studies to construct

predictive models of surgical outcome, aiding clinical teams during patient pre-surgical evaluations.

Introduction

Focal epilepsy is characterised by recurrent, unprovoked seizures believed to originate from an "epileptogenic zone" within a single cerebral hemisphere[1]. For people living with drug resistant focal epilepsy, the goal of surgical resection is to remove this epileptogenic zone. At present, surgical intervention fails to completely suppress seizures in 30-40% of cases[2]. However, for patients with focal neocortical epilepsy the chance of post-operative seizure freedom is even lower[2,3].

Currently, it is not fully understood why some patients with neocortical epilepsy have unfavourable surgical outcomes, although some mechanisms have been proposed. Englot et al.[4] reviewed surgical outcome for 125 patients with focal neocortical epilepsy. Suggested reasons for surgical failure include incorrect localisation, incomplete resection of the epileptogenic zone, or the presence of a secondary distant epileptogenic zone. Additionally, higher seizure frequency, history of secondary generalised seizures, and normal MRI were associated with worse post-operative outcome. These results were consistent with those reported by Bell et al.[5]. Other studies suggest that the development of new epileptogenic zones post-operatively[6], and the presence of more widespread distributed epileptogenic networks[7] may also relate to surgical failure.

Multiple mechanisms could lead to poor surgical outcome in terms of seizure freedom (considered as surgical failure), with different mechanisms likely in different patients[8]. One mechanism is mislocalisation of the epileptogenic zone, which would mean a failure to resect epileptogenic abnormalities. A mislocalised resection is unlikely to suppress patient seizures and could introduce additional comorbidities post-surgically. Second, a partial resection of the epileptogenic zone may improve seizure severity or frequency but, with some remaining epileptogenic tissue, it is unlikely that total seizure freedom will be achieved. These first two mechanisms view the epileptogenic zone as a localised region/cluster of abnormal tissue. However, in some patients, a third mechanism by which poor outcomes could arise is if abnormalities remain post-surgically. Such widespread abnormalities would likely be less impacted by a localised resection, and therefore lead to poorer outcomes. Although the mechanisms of surgical failure may differ from one patient to another, a central concept is that of the epileptogentic zone – a presumably abnormal area, which is indespensible for seizure generation[9] and thus should be targeted during surgical resection.

To help localise the epileptogenic zone and predict surgical outcome, previous studies used pre-operative resting-state MEG data[10–14]. These studies typically focused on patient data only without incorporating normative data from healthy controls into the analysis. Without accounting for the normative variations in health, it is difficult to identify abnormalities. Relating abnormalities relative to health with surgical outcome has been fruitful using structural MRI data[15–18]. However, this normative approach is rarely used for functional/neurophysiological data, despite efforts to promote these methods[19–21]. Recently, Taylor et al.[22] derived invasive intracranial EEG band power normative maps using interictal resting-state recordings. Using those maps as a baseline, the authors computed abnormality maps for 62 patients with epilepsy and related them to surgical outcome. In patients with poor surgical outcome, spared tissue was more abnormal than the resected tissue. The accurate localisation of the epileptogenic zone using pre-operative MEG data has been shown to relate to surgical outcome. To our knowledge, a normative approach similar to that used by Taylor et al[22] to localise the epileptogenic zone has not been applied using noninvasive neurophysiological data, such as MEG.

In this study, we propose three mechanisms of surgical failure, in terms of post-operative seizure relapse. These mechanisms are 1) failing to resect abnormalities, 2) partial resection of the epileptogenic zone, and 3) local resections insufficiently altering the global cortical abnormality. We develop quantitative markers for each surgical failure mechanism using interictal MEG band power abnormality maps for 32 individuals with neocortical epilepsy with 70 healthy controls as a normative baseline. We demonstrate that when combined, these markers of surgical failure mechanisms discriminated outcomes well (AUC=0.82, p=0.0008). These mechanisms shed insight to the reasons for surgical failure and serve as markers for predictions of outcomes.

Methods

Patients and controls

Data were acquired pre-operatively for 32 individuals with refractory neocortical epilepsy and 70 healthy controls. All patients later underwent neocortical surgical resection as determined following pre-surgical evaluation. Additional to the 32, a further 19 patients with temporal lobe epilepsy underwent surgery for resection of the hippocampus and are included in the supplementary materials for completeness. Hippocampal resection patients are not included in the main text as our MEG processing did not include deep brain structures, including the hippocampus. Surgery outcome was assessed 12 months post-operatively with patients classified using the ILAE definition of seizure freedom[23]. Inclusion criteria for the study were patients with preoperative MRI and MEG, along with postoperative MRI and seizure outcome available at least 12 months. Standard statistical tests were used to quantify any differences between control and patient sub-groups for commonly collected clinical demographics. The results of the statistical comparisons are summarised in table 1. For categorical demographics (resection hemisphere and history of focal to bilateral tonic clonic seizures), two-tailed χ^2 tests were performed. Continuous demographics (age, age of onset, epilepsy duration) were compared using two-tailed two sample t-tests.

	Controls (1)	ILAE 1 (2)	ILAE 2+ (3)	Test statistic
N	70	12	20	
Age (mean, SD)	26.9 (6.9)	32.3 (10.7)	32.3 (11.3)	$P_{1,2} = 0.058, t = 2.085$ $P_{1,3} = 0.057, t = 2.003$ $P_{2,3} = 0.807, t = -0.247$
Sex (Male, Female)	27, 43	7, 5	10, 10	$P_{1,2} = 0.334, \chi^2 = 0.935$ $P_{1,3} = 0.510, \chi^2 = 0.434$ $P_{2,3} = 0.927, \chi^2 = 0.008$

Age onset (mean, SD)	N/A	9.7 (7.6)	12.3 (6.8)	$P_{2,3} = 0.356$, $t = 0.945$
Epilepsy duration (mean, SD)	N/A	23.6 (10.0)	20.0 (8.8)	$P_{2,3} = 0.333$, $t = -0.992$
Resection hemisphere (Left, Right)	N/A	6, 6	11, 9	$P_{2,3} = 0.927$, $\chi^2 = 0.008$
Focal to bilateral tonic clonic seizures (Yes, No)	N/A	6, 6	16, 4	$P_{2,3} = 0.168$, $\chi^2 = 1.901$

Table 1: Summary of patient and control data demographics. *Statistical comparisons are made using two-sample t-tests for continuous variables and χ^2 tests for categorical variables. Two-tailed statistical tests were performed as no clear hypothesis of direction was provided.*

MRI acquisition and pre-processing

T1 weighted MRI was performed using a 3T GE Signa HDx scanner (General Electric, Waukesha, Milwaukee, WI). Acquisition details for patients have been previously reported[24] (acquired in London), and for healthy controls[25] (acquired in Cardiff). Subject MRI scans were pre-processed using the standard Freesurfer pipeline 'recon-all'[26]. MRI scans were parcellated into cortical regions of interest (ROIs) based on the Lausanne parcellation scheme for four different resolutions (68, 114, 219 and 448 cortical ROIs)[27].

To identify patient specific resection cavities, pre and post-operative MRI scans were linearly coregistered using the FSL tool 'FLIRT'[28–30]. Using FSLview, pre and post-operative MRI were overlaid, with resection volumes manually drawn. Following this, pre and post-operative ROI volumes were calculated using custom MATLAB code[24]. Regions were categorised as resected if the pre and post-surgical volume change exceeded 10%. Regions with volume changes between

1-10% were categorised as 'Unknown' and were subsequently removed from any analysis. The threshold classifying whether regions were resected was scanned between 1-25% with no substantial differences in the results.

MEG acquisition and pre-processing

Eyes-closed resting-state MEG recordings were acquired for patient and healthy cohorts using a 275 channel CTF whole head MEG system in a magnetically shielded room. Patient data were collected during pre-surgical evaluation at UCL in London. Healthy control normative data were collected as part of the MEG UK partnership at CUBRIC, Cardiff. Raw MEG recordings were pre-processed using Brainstorm[31]. First, MEG sensor locations and structural MRI scans were co-registered using the fiducial points. The quality of co-registration was visually inspected and refined if required. Second, MEG recordings were downsampled to a sampling frequency of 600Hz and bandpass filtered between 1-100Hz to reduce the computational cost. Recordings were subsequently filtered at 50Hz using a second order IIR notch filter with 3-dB bandwidth to remove powerline artifacts. Cardiac and ocular artifacts were identified and manually removed using independent component analysis (ICA) after channel recordings were dimensionally reduced to 40 components using principal component analysis (PCA).

Following artifact removal, MEG data was source reconstructed using the minimum norm estimate approach, sLORETA, coupled with an overlapping spheres head model. This resulted in 15000 sources constrained perpendicular to the cortex. Sources were downsampled into neocortical ROIs based on the Lausanne parcellation scheme for four different resolutions[27]. Note that, due to low signal to noise and their complex geometry, deep brain subcortical volumetric structures of the Lausanne atlas were not included. Specifically, we excluded the hippocampus and amygdala, amongst others, from our analysis entirely. Within the main text we therefore only present results for patients who had resections to neocortical tissue where complete MEG coverage was present. We include patients with hippocampal resections in supplementary for completeness. Source recordings within each ROI were sign flipped and averaged, resulting in a single time series per region. Finally, subject time series were reduced to 70 second epochs of continuous recordings, clear of any residual artifacts (figure 1.A). Recordings were not inspected for interictal spikes here as occasional epileptic spikes have little, to no effect on the regional power spectral densities and maximum abnormality estimates[22].

Normative mapping of MEG band power

Neocortical regional power spectral densities were computed using Welch's estimate, with a 2 second sliding window and 50% overlap between consecutive windows. Absolute band power was estimated for five commonly used frequency bands, delta (1-4Hz), theta (4-8Hz), alpha (8-13Hz), beta (13-30Hz), and gamma (30-80Hz) (figure 1.B). For gamma, 47.5-52.5Hz were excluded to mitigate any residual artifacts caused by UK powerlines. Absolute band power estimates were scaled by the total power across all frequencies to obtain the relative contributions within each band. Normative maps were constructed by taking the control cohort average relative band power within each region and frequency band (figure 1.C).
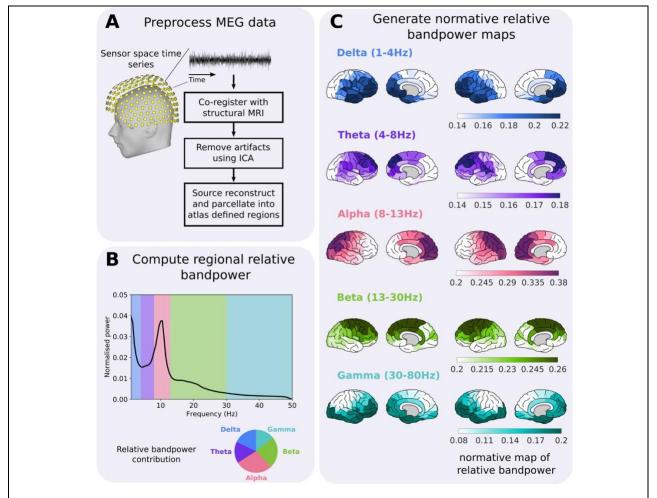

Figure 1: Pre-processing pipeline for normative MEG recordings. *First, **(A)** MEG recordings were pre-processed to remove any artifacts due to powerline interference, or cardiac and ocular events. After artifact removal, 70 second epochs of channel recordings were source reconstructed and downsampled into cortical regions based on the Lausanne parcellation. Second, **(B)** regional power spectral densities were computed for each patient. The relative*

band power contribution was calculated for five commonly used frequency bands: delta (1-4Hz), theta (4-8Hz), alpha (8-13Hz), beta (13-30Hz), and gamma (30-80Hz). For gamma 47.5-52.5Hz were discarded to minimise any residual effects due to powerline artifacts. Note the x-axis terminates at 50Hz for illustrative purposes only. Finally, (C) regional band power contributions were averaged across the cohort to create normative maps of relative band power for each of the five frequency bands.

Abnormality mapping of patient MEG band power

Similar to healthy controls, relative band power contributions were computed for the patients with epilepsy. For each region and frequency band, the absolute z-score was computed using healthy controls as a baseline. Abnormalities were computed for each individual using equation 1, where i corresponds to the region of interest, j the frequency band, and $\mu_{i,j}$, $\sigma_{i,j}$ the mean and standard deviation of the healthy controls respectively. To reduce the dimensionality, maximum absolute z-scores across frequency bands were retained for each region. Dimension reduction accounts for the heterogeneity of abnormalities across regions and patients, resulting in a single band power abnormality map per patient. Estimation of abnormality maps are illustrated in figure 2.A.

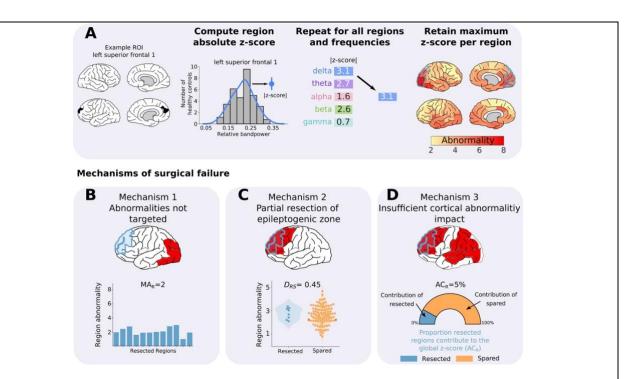$$| z_{i,j} | = \left| \frac{x_{i,j} - \mu_{i,j}}{\sigma_{i,j}} \right| \qquad (1)$$

Figure 2 : Processing pipeline for patient abnormality mapping and derivation of the three surgical failure mechanisms. (A) *Patient abnormality maps were generated using control data as a baseline **(top panel)**. For each region and frequency, the band power contribution was z-scored using control data as a reference. Within each region, frequency abnormality dimensions were reduced by only retaining the maximum absolute abnormality. This process was repeated for all regions to create patient specific maps of band power abnormalities. Three mechanisms were proposed which could underlie surgical failure **(bottom row)**. **(B)** First, failure to resect abnormalities could lead to poor surgical outcome. This mechanism was quantified using the average abnormality of the resected tissue (MA_R), with lower values hypothesised to cause surgical failure. **(C)** Second, we hypothesised that a partial resection to the epileptogenic zone regardless of whether abnormalities are resected, could lead to surgical failure. To quantify this mechanism, we used D_{RS} scores to measure the separability of the resected and spared tissue based on abnormality values. D_{RS} is identical to the AUC. Scores close to 0 indicate that the abnormalities of resected tissue are greater in magnitude than abnormalities of spared tissue. Conversely, D_{RS} scores close to 1 indicate that the spared tissue is more abnormal relative to the resected tissue. **(D)** Finally, insufficient cortical abnormality impact could also contribute to a poor surgical outcome. We quantified this mechanism using AC_R, defined as the abnormality contribution of resected tissue, relative to the global abnormality. If abnormalities are widespread, the overall cortical abnormality is unlikely to be sufficiently altered by a localized resection, potentially leading to surgical failure.*

Mechanisms of surgery failure

We proposed three mechanisms which could relate to surgical failure in patients with neocortical epilepsy. Each mechanism was quantified using the patient specific band power abnormality maps. First, failing to target abnormalities likely contributes to a poor surgical outcome (figure 2.B). That is, if the resection area is seemingly normal (i.e. similar to the control data) we hypothesised that there would be a poor surgical outcome. We quantify this mechanism using the mean abnormality of the resection (MA_R), which corresponds to the mean absolute z-score of the resected regions. We hypothesised that patients with lower magnitude resection abnormalities would be less likely to be seizure-free postoperatively.

Our second proposed mechanism of post-operative seizure recurrence is the partial resection of the epileptogenic zone. Abnormal tissue may be resected, but if other, more abnormal tissue is spared an unfavourable surgical outcome may be more likely (figure 2.C). To quantify this mechanism we use the distinguishability measure D_{RS}. Introduced by Wang et al.[32], the D_{RS} is synonymous to the area under the receiver operating characteristic curve (AUC). Ranging between 0 and 1, D_{RS} scores closer to 0 indicate that the most abnormal regions are resected. Conversely, values close to 1 indicate that the most abnormal regions are spared. D_{RS} scores close to 0.5 correspond to chance, with no discernible difference between the z-scores in the resected and spared tissue.

Finally, we propose that insufficiently impacting the cortical abnormality during resection may also contribute to surgical failure (figure 2.D). If high magnitude abnormalities remain across the cortex it is unlikely that a localised resection of abnormal tissue, even the most abnormal tissue, will sufficiently alter the overall global abnormality. We use the abnormality contribution of resected tissue on the global abnormality (AC_R) as a marker for this mechanism. This marker corresponds to the proportion resected tissue contributes to the overall absolute z-score. The AC_R is bound between 0-100%, with larger values indicating that the resection more heavily contributes to the global abnormality.

Statistical testing

Surgical outcome discriminability of surgical failure mechanisms

To assess how well our three proposed mechanisms explain surgery outcome (ILAE 1 vs ILAE 2+) we computed AUC scores, with specific hypotheses on the directions of our observed effects.

We hypothesised that the resections of seizure free patients would be more abnormal than patients with continued seizures. Furthermore, we hypothesised that patients with favourable outcomes would have lower D_{RS} scores and higher AC_R scores in comparison to poor outcome patients. Corresponding p-values were estimated using the Mann-Whitney U test, an unscaled version of the AUC statistic. A non-parametric alternative to an independent two sample t-test, the Mann-Whitney U test assesses whether the rank order of samples from two independent distributions significantly differ. One-tailed tests were performed as clear hypotheses of direction for each mechanism are provided.

We also postulated that the MA_R and D_{RS} of seizure free patients differed significantly from preconceived thresholds. One-tailed, one sample Wilcoxon signed-rank tests were used to assess whether patients significantly differed from each threshold. For D_{RS}, we hypothesised that seizure free patients were significantly less than chance ($D_{RS} < 0.5$). Additionally, we hypothesised that the MA_R was significantly greater than health in seizure free patients. To test this hypothesis, a threshold was set at | z-score |$= 2.6$ based on the results of a simulation study. Five samples were randomly drawn from a standard normal distribution to simulate relative band power abnormality for each frequency band within a single cortical region. We repeated this 100,000 times, retaining the maximum absolute z-score at each iteration. This resulted in 100,000 samples of maximum absolute z-scores drawn from a standard normal distribution. A threshold of 2.6 corresponds to the 5% significance level. At the 1% and 0.1% significance levels the thresholds are set to | z-score |$= 3.0$ and | z-score |$= 3.7$ respectively. An analogous simulation for one sample, instead of five, would lead to 1.96 threshold representing the 5% level. We used a one tailed one sample Wilcoxon signed rank test, hypothesizing that seizure free patients would be greater than 2.6.

Comparisons with clinical demographics

Clinical demographics can be used during the pre-surgical evaluation as predictors of surgical outcome[33]. We postulated that our mechanisms of surgical failure perform at least as well as clinical demographics for surgical outcome separation. A random sample of 32 patients with replacement was chosen from our cohort of patients, and corresponding AUC's were computed for each of the three mechanisms and clinical variables. This procedure was repeated 1000 times to produce distributions of AUC scores for each feature. The mean and standard deviation were recorded and compared between mechanisms and clinical demographics.

Simultaneous analysis of surgical failure mechanisms

As surgical failure is multifactorial, with numerous paths leading to surgical failure, analysis of each mechanism individually is likely to underperform when identifying poor surgical candidates. Instead, a unified analysis of all mechanisms may identify more candidates unsuitable for surgical intervention as more of the variability is accounted for. To unify all mechanisms into a single analysis, the optimal surgical outcome separability threshold for each was calculated.

Optimal mechanism thresholds were identified using the receiver operating characteristics curves previously computed to obtain AUCs. Each curve is comprised of pairs of true positive and false positive rates (TPR and FPR respectively) estimated for a series of different threshold values. The optimal threshold to distinguish outcome groups is located at the point which optimally maximises the TPR, whilst simultaneously minimising the FPR. This point corresponds to the maximum geometric mean of the TPR, FPR rates, highlighted by equation 2, in which n corresponds to the number of value pairs. For poor surgical candidates the MA_R and AC_R measures which correspond to failing to resect abnormalities and insufficiently impacting cortical abnormalities respectively are more likely to subceed the selected threshold. Conversely, for poor outcome patients with suspected partial resections to the epileptogenic zone we could expect the D_{RS} to exceed the threshold.

$$\max\left(\sqrt{TPR_i \times (1 - FPR_i)}\right) \ for \ i \ in \ 1 \cdots n \ (2)$$

Code and data availability

All analysis was performed in Python version 3.6.9. Surface plots were created in MATLAB R2019b using the simple brain plot repository[34]. Code and data to reproduce the figures in the manuscript will be made available upon acceptance of the manuscript.

Results

Normative mapping of MEG band power

We generated normative MEG band power maps for five frequency bands. Figure 1.C highlights the spatial distribution of relative cortical band power averaged across the cohort of 70 healthy controls. MEG derived normative maps exhibited spatial distributions in agreement with previous literature. For example, strong delta activity was observed in ventral frontal regions bilaterally, as well as strong alpha activity in parietal and occipital regions. We compared our MEG normative maps to those derived using intracranial EEG[22] (supplementary S1.1) and found strong associations across these modalities for most frequency bands (figure S1). Notable differences are observed in the theta (Pearson R=0.36) and gamma (Pearson R=-0.2) frequency bands.

Markers of surgical failure mechanisms differ across poor outcome patients

We proposed three intuitive mechanisms that could contribute to surgical failure. Each mechanism was quantified using patient specific band power abnormality maps. To illustrate the importance of each mechanism and their association with surgical failure, we provide examples using three patients with unsuccessful surgical interventions (figure 3).
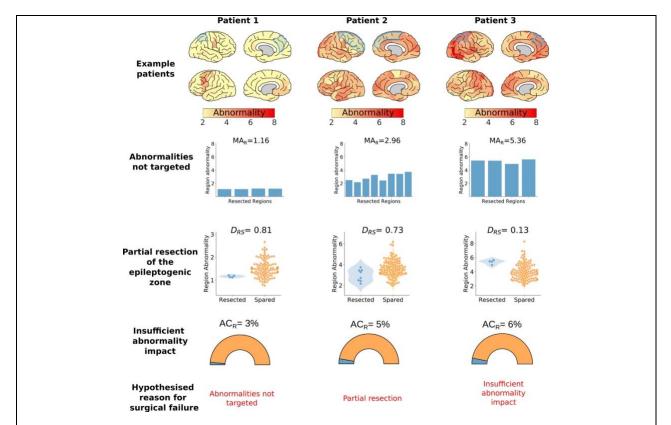
Figure 3: Mechanism results for three example poor outcome (ILAE 2+) patients *The top row shows patient cortical abnormality maps, with subsequent resections in blue. Lower rows show the markers for each of the three proposed mechanisms of surgical failure. Each column corresponds to a different patient, illustrating the variety of pathways (consisting of one or more mechanisms) which could lead to a surgical failure. For patient 1 **(left column)**, it is evident that abnormalities were not resected, with an average resection abnormality of 1.16. As such, it is likely that the failure to resect abnormalities contributed towards the patient's poor surgical outcome. For patient 2 **(centre column)**, abnormalities were resected but the most abnormal tissue was spared ($D_{RS} = 0.73$) suggesting the epileptogenic zone may have been partially resected. The corresponding abnormality map illustrates that widespread abnormalities were present, a confounder which may have led to the failed surgical intervention. Finally, for patient 3 **(right column)**, although some of the most abnormal cortical tissue was resected, other abnormalities were widespread. As such, the global abnormality was likely not sufficiently altered ($AC_R = 6\%$). All three patients fail at least one of our proposed mechanisms.*

We first postulated that failing to resect abnormal tissue is likely related to a poor surgical outcome. For patient 1 (figure 3, left column) the mean abnormality of the resection is low (MA_R=1.16), suggesting that most of the resected tissue is normal. Indeed, the possibility of mislocalisation is apparent upon visual inspection of the corresponding abnormality map (figure 3, top row, left

panel). Strong abnormalities are only present in the contralateral hemisphere in the left frontal lobe. For this reason, we hypothesised that the patient's right parietal lobe resection would not lead to post-operative seizure freedom. Conversely, patients 2 and 3 had favourable MA_R scores, with values of 2.96 and 5.36 respectively, suggesting that their resection *did* target abnormal - potentially epileptogenic - tissue.

Second, we hypothesised that regardless of whether the epileptogenic zone was localised, surgical outcome will be poor if the epileptogenic zone was only partially resected and other more abnormal regions remained. We propose that sparing the *most* abnormal tissue, regardless of resection abnormality, as a marker for the second mechanism of surgical failure. The marker used for the second mechanism of surgical failure is the metric D_{RS}, which quantifies if the spared tissue is more abnormal than the resected tissue. Values close to 1 suggest that abnormalities were spared by surgery. Patient 2, measured $D_{RS} = 0.73$, which suggests that although possible epileptogenic abnormalities were targeted, some remaining epileptogenic tissue may have been spared. Thus, we would hypothesise a poor surgical outcome for the second patient.

For the third proposed mechanism, patient 3 demonstrated favourable markers for the first two proposed mechanisms (figure 3, right column), with an MA_R of 5.36 and D_{RS} of 0.13. Based on these findings, one may expect a good outcome. However, the markers for the targeting of abnormalities and partial resection of the epileptogenic zone both fail to directly account for abnormalities beyond the resection. If abnormalities are widespread across the cortex, it is unlikely that resecting the most abnormal tissue will completely suppress seizures. Our third marker of surgical failure, AC_R, accounts for the abnormalities in spared tissue by quantifying the proportion that resected abnormalities contributed to the overall global abnormality. For patient 3, the AC_R highlights that only 6% of the global abnormality was resected. The low contribution of the resection to the overall abnormality leads us to suggest that the localised resection was insufficient, thus leading to a poor surgical outcome.

In contrast to the non seizure free patients in figure 3, figure 4 highlights the markers for a patient with good surgical outcome. Patient 4 has no markers of surgical failure. First, the resection targeted abnormal tissue with an MA_R of 5.95 (figure 4.B), indicating the epileptogenic zone was likely correctly localised. Moreover, a D_{RS} of 0.1 indicates that the most abnormal tissue was removed, suggesting that the whole epileptogenic zone may have been resected (figure 4.C).

Finally, we observed that the localised resection had a strong impact on the global abnormality, with an AC_R of 19% (figure 4.D). Altogether, the results for this patient would indeed suggest a good surgical outcome based on the chosen resection site.
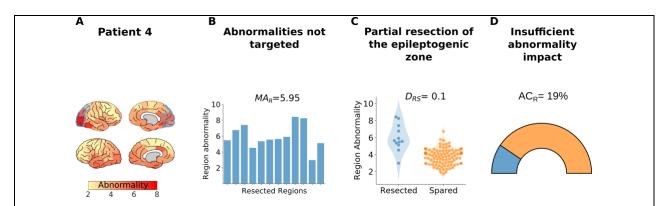

Figure 4: Mechanism results for an example good outcome patient. (A) Patient 4 underwent resective surgery, achieving total seizure suppression 1 year post-operatively. For all three mechanisms, patient 4 passes criteria to suggest surgical success. (B) First, abnormal tissue has been targeted within the resection cavity. (C) Additionally, it is clear that the most abnormal cortical tissue has been targeted. (D) Finally the AC_R suggests that the overall cortical abnormality may have been sufficiently altered after resection. Together, these results based on pre-operative interictal MEG recordings would lead us to hypothesise that the proposed resection zone for this patient is sufficient to completely suppress seizures.

Markers of surgical failure mechanisms discriminate outcome groups

In this section we applied markers of the three surgical failure mechanisms to the entire cohort of 32 neocortical epilepsy patients. Each marker was derived using patient abnormality maps with healthy controls as a baseline. As abnormalities were computed across frequency bands and regions there is a potential for large abnormalities to be observed by chance. We therefore checked whether the MA_R scores were significantly greater than what we would have expected to see by chance. We also quantified the overall performance of each marker to distinguish surgical outcome groups. Cohort-wide associations between our markers of surgical failure and surgery outcome are reported in figure 5.
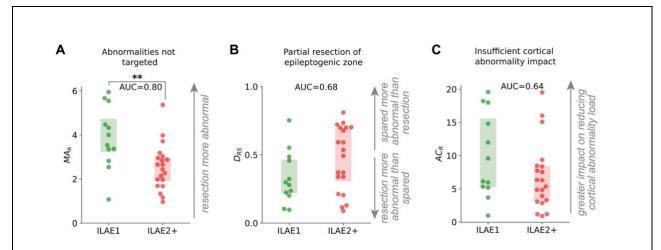
Figure 5: Surgical outcome separability of each mechanism at the group level. *Boxplots illustrate how well each mechanism discriminates surgical outcome groups. Each datapoint represents an individual patient. Boxes extend from the 25th-75th% of the data. For each mechanism, the AUC is calculated along with corresponding p-value using a one-tailed Mann-Whitney U test. Good outcome patients (ILAE 1) are depicted in green, and bad outcome (ILAE 2+) in red. (**) corresponds to statistical significance at the 1% level.*

For the MA_R scores, which correspond to the targeting of abnormal tissue (figure 5, left), we see that the MA_R scores of seizure-free (ILAE 1) patients are larger than those of non seizure free (ILAE 2+) patients (AUC=0.80, p $= 0.003$). This result highlights that resections with stronger abnormalities are associated with surgical success. Further, the MA_R scores for seizure free patients differ from health at the 5% and 1% levels ($MA_R > 2.6$,W=70.0, p $= 0.006$ and $MA_R > 3.0$,W=64.0, p $= 0.026$ respectively). Meanwhile, our marker for the partial resection of the epileptogenic zone, D_{RS} was larger in patients with poor surgical outcome (AUC=0.68, p $= 0.053$). That is, in poor outcome patients the most abnormal cortical tissue was typically spared rather than resected (figure 5, centre). Moreover, D_{RS} scores for good outcome patients were less than chance $D_{RS} = 0.5$ (W=10.0, p $= 0.010$), meaning that resected regions were more abnormal than spared. Finally, our third marker corresponding to insufficiently altering the global abnormality (AC_R) was larger in good outcome patients. This marker quantifies the impact that the resection has on the overall abnormality load (figure 5, right). This effect is in the hypothesised direction, being a larger impact in seizure-free patients (AUC=0.64, p=0.096).

These results show that, as in our example patients, our markers of surgical failure mechanisms may identify patients with poor surgical outcomes across the cohort studied.

19

Comparison with clinical demographics

Prior to surgical intervention, patients undergo a pre-surgical evaluation to determine if they are suitable candidates for the procedure and which tissue should be resected. Clinical demographic information may be used to aid decision making during the pre-surgical evaluation, and can hold predictive information[33]. We therefore next compared the performance of our markers of surgical failure mechanisms to clinical demographics to assess how well they distinguish surgical outcome groups (figure 6). We found that age at resection, duration of epilepsy, and hemisphere of resection did not distinguish surgical outcome groups well, with mean AUCs of 0.45, 0.39 and 0.47 respectively. Age of epilepsy onset and history of focal to bilateral tonic-clonic seizures were moderately associated with surgical outcome with AUCs of 0.62 and 0.65 respectively. All three of our markers of surgical failure mechanisms distinguish outcome groups above and beyond chance (Abnormalities not targeted: $\overline{\text{AUC}} = 0.79$, Partial resection of the epileptogenic zone: $\overline{\text{AUC}} = 0.67$, Insufficient cortical abnormality impact: $\overline{\text{AUC}} = 0.64$), matching or exceeding the separability of the clinical demographics.
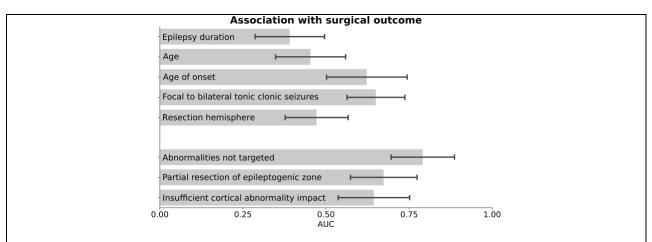

Figure 6: Surgical outcome separability comparisons between clinical demographics and mechanisms of surgical failure. *Each bar corresponds to the AUC obtained when comparing surgical outcome groups using each variable individually. Bootstrapping with 1000 repeats is performed, with each bar corresponding to the average surgical outcome AUC. Error bars show the 95% confidence interval for each variable.*

Simultaneous analysis of surgical failure mechanisms relates to post-surgical outcome

Epilepsy is heterogeneous, with a wide range of mechanisms by which seizures may originate and manifest. It is therefore reasonable to assume there are multiple mechanisms which render treatment ineffective, with different mechanisms at play in different patients. Analysing each mechanism independently would thus likely underperform for surgical outcome prediction relative to a unified analysis as each explains unique causes for surgical failure. The different impact of each mechanism on patients is evident in section 3.2, as each patient presented with different markers of surgical failure. Patient 1 had three markers of surgical failure based on our proposed mechanisms (figure 3.2, left column), patient 2 had two markers (figure 3.2, middle column), whereas patient 3 only had one marker (figure 3.2, right column), yet all had post-surgical seizures. This motivated us to assess the degree of similarity between mechanisms, and analyse the joint performance of all mechanisms for distinguishing patient outcomes. We hypothesised that a combined analysis would increase the proportion of patients correctly identified as poor surgical candidates.

The three proposed mechanisms of surgical outcome failure provided complementary information, with Pearson correlations of R=-0.64 between the MA_R and D_{RS}. The correlation between the MA_R and AC_R was R=0.39 and R=-0.37 between the D_{RS} and the AC_R (figure S2). Given this complementary information, optimal thresholds to discriminate surgical outcome groups were next chosen based on a data driven approach (methods section 2.7.3). A patient would be considered a poor surgical candidate if the mean abnormality of the resected tissue (MA_R) was less than 3.35. For patients with partial resections to the epileptogenic zone or insufficient impact to the cortical abnormality we would expect to see a $D_{RS} > 0.34$ or $AC_R < 9.58\%$ respectively. Some 17 out of 20 (85%) non seizure free patients had MA_R scores less than 3.35. Similarly, 85% of non seizure free patients had AC_R values less than 9.58%. For non seizure free patients 15 out of 20 (75%) had D_{RS} scores greater than 0.34 a marker of surgical failure due to the partial resection of the epileptogenic zone. Combining all mechanisms into a single analysis showed that 19 of the 20 (95%) non seizure free patients were identified with at least one marker of surgical failure, figure 7.
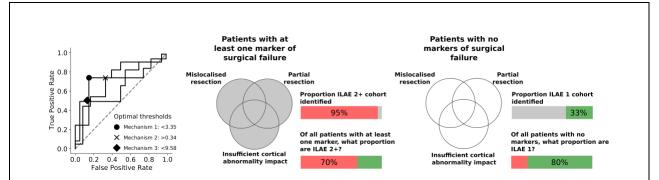
Figure 7: Harmonisation of all three mechanisms into a single analysis. *ROC curves **(left)** for each mechanism are used to identify the optimal threshold which discriminates the two surgical outcome groups. Optimal thresholds are selected at the point which maximises the true positive rate whilst simultaneously minimising the false positive rate. Patients are filtered into sub groups based on those that fail to meet the criteria for at least one mechanism **(centre)** and those that pass all three mechanisms **(right)**. Shaded areas (grey) of Venn diagrams illustrate the criteria used to filter the cohort. Specificity corresponds to the proportion of good or bad outcome patients identified relative to all patients identified for the corresponding criteria.*

In total, 27 patients had at least one marker of surgical failure, of which 70.37% went on to have poor surgical outcomes. Moreover, 90%, and 60% of poor outcome patients had two and three markers of surgical failure respectively. Contrarily, seizure free patients had one, two, and three markers of surgical failure with rates of 66%, 25%, and 16% respectively. Using the number of markers of surgical failure we found that the unified analysis distinguishes surgical outcome groups well, AUC=0.82, p=0.0008. For patients where our confidence of post-operative seizure-freedom was highest (i.e. no markers of surgical failure), we were correct in 4 out of 5 cases, with the remaining patient later recovering from year two. To summarise, if a patient failed at least one marker, there is a 70% chance of poor outcome. In contrast, if a patient passed all three markers, there is a 80% chance of good outcome.

Discussion

Different patients may have different reasons for post-surgical seizure recurrence. In this study we proposed three mechanisms which could relate to epilepsy surgical failure. Each mechanism was quantified using patient-specific band power abnormality maps derived from interictal MEG recordings, acquired as part of a pre-surgical evaluation. First, we demonstrated that each marker of the surgical failure mechanisms relates to surgical outcome in the hypothesised direction, with the resection of abnormalities (MA_R) significantly separating outcome groups (AUC=0.80, p=0.003). Second, we show that our proposed mechanisms perform better than clinical demographics commonly used as part of a routine pre-surgical evaluation. Finally, by identifying optimal thresholds of separability, we showed that 95% of non seizure free patients (ILAE 2+) had at least one marker of surgical failure, suggesting our mechanisms could be beneficial during the pre-surgical evaluation.

Our work introduces mechanisms of surgical failure which could be clinically useful. Both intuitive, and easy to quantify, each mechanism provides important insights into why some patients fail to completely suppress seizures post-operatively. First, we hypothesised that not targeting abnormal, possibly epileptogenic tissue would result in surgical failure. This mechanism builds upon the extensive literature relating structural abnormalities of the resected tissue to surgical outcome[15–18,24]. We quantified this mechanism as a single value per patient using the mean resection abnormality (MA_R). Our results suggest that the resection of abnormalities (MA_R) is indeed crucial for post-operative seizure control, and that normative mapping can serve as a useful way to identify abnormalities.

Next, it is conceivable that the resection may indeed remove abnormal tissue, but that other, even more abnormal areas remain (e.g. in eloquent cortex). Our measure for the possible mislocalisation of epileptogenic tissue only measures properties of resected regions, disregarding remaining tissue. We therefore postulated that for patients with partial resections to the epileptogenic zone regardless of resection abnormality, if the most abnormal tissue is spared, then only partial seizure suppression is expected. We quantified the partial resection using the D_{RS}[32,35], a measure which captures whether resected tissue is more abnormal than spared. Consistent with results reported by Taylor et al.[22], we show that this mechanism relates to outcome in the hypothesised direction (AUC > 0.5). Moreover, the resection of the most abnormal tissue in seizure free patients was

significantly more common than chance ($D_{RS} < 0.5$), suggesting these regions were not randomly targeted during surgical intervention, but correctly identified in seizure free patients. In contrast, D_{RS} scores for non seizure free patients were not significantly different than chance, indicating the most abnormal tissue was not removed in those patients. Supporting our findings, Englot et al.[4] reported that surgical intervention did not completely suppress seizures in 72% of the non seizure free patients (ILAE 2+) because the epileptogenic zone was only partially resected. Similarly, Kim et al.[36] also reported that complete resection of the ictal onset areas, identified by frequent interictal spiking during an intracranial EEG study, related to better surgical outcome for a cohort of 109 neocortical patients.

The two proposed mechanisms of surgical failure thus far focus primarily on the resection, with little consideration of the abnormalities in surgically spared tissue. We introduced a third mechanism to identify whether strong abnormalities are present beyond the proposed resection, using the AC_R as the marker of surgical failure. We hypothesised that if strong cortical abnormalities exist beyond the proposed resection site, a localised resection may not be sufficient to completely suppress seizures post-surgically. Widespread abnormalities for individuals with epilepsy have previously been reported using diffusion MRI data[37,38], with some attributing widespread abnormalities to an underlying epileptogenic network facilitating the spread of seizures to distant regions[9,39]. Our marker of surgical failure may reflect this underlying epileptogenic network, though further markers derived using functional connectivity matrices are required to confirm this hypothesis. Together, our three mechanisms account for abnormalities within both the resected and spared tissue, providing clinicians additional insight into the proposed resection site for each individual patient.

In isolation, each mechanism discriminates surgical outcome groups in the hypothesised directions, with the targeting of abnormalities significantly discriminating outcome groups (figure 5). Yet, each proposed mechanism provides valuable information in the context of surgical failure. As reported previously[4], surgery failures may occur for different reasons, and so it is unlikely for a single mechanism to fully distinguish surgical outcome groups. Our formalism of these surgical failure mechanisms allowed us to demonstrate that 95% of poor outcome patients presented with at least one marker of surgical failure, 90% with at least two markers, and 60% with markers of surgical failure for all three mechanisms. Overall, a combination of all three mechanisms

discriminated surgical outcome groups well (AUC=0.82,p=0.0008). Fourteen patients were identified with three markers of surgical failure and thus would be hypothesised to be poor surgical candidates. In reality, 86% of those patients with three markers of surgical failure were indeed not seizure free post-surgically. In total five patients had no markers of surgical failure based on our proposed mechanisms, thus suggesting good outcome for all five. Indeed, four of those were seizure-free, with the remaining patient ILAE 3 at 12 months. However, that patient experienced only one seizure whilst in the process of reducing their medication dose during their first months post-surgery. Although initially poor outcome due to the solitary seizure in year 1, this was an isolated incident and the patient was seizure free for all subsequent years of follow up (over 5 years to date). Our results suggest that the analysis of these surgical failure mechanisms, using a multimetric framework, may provide robust predictions of surgical outcome of use during pre-surgical evaluation.

While we have proposed three mechanisms of surgical failure, others may exist, including the presence of multiple epileptogenic foci, or the development of new epileptogenic zones post-operatively. To assess whether multiple foci are present, spatial statistics could be used[40,41]. Spatial statistics could allow investigation of spatial organization of abnormalities, and their proximity to the resection. Such approaches could be useful for recognising previously unidentified multifocal abnormalities, which may be a contraindication for surgery. To investigate the development of new epileptogenic zones post-operatively, an extension into network based statistics for structural and functional data could be beneficial. Recently, it has been proposed that there exists widespread post-surgical functional abnormalities that were not present pre-surgically[6]. There, the authors hypothesised that post-surgical evolution of the epileptogenic process may have contributed to continued seizures in poor outcome patients. In addition, a longitudinal study of 48 patients following temporal lobe resections revealed greater white matter post-operative changes related to better outcomes[42]. In summary, future studies could develop markers pertaining to new mechanisms of surgical failure and incorporate them with our mechanisms for a more comprehensive analysis.

Although applications to pathology such as epilepsy are rare, normative mapping of relative band power has been reported previously[19,22,43–49]. Our normative maps of band power illustrate strong bilateral delta activity in ventral frontal tissue, and strong bilateral theta activity in dorsal frontal

regions. Furthermore, our maps show strong bilateral alpha activity in occipital and parietal tissue. Niso et al.[46] report similar spatial distributions using resting-state MEG recordings from 46 healthy controls. Interestingly, we found that spatial distributions of normative band power are consistent across modalities. Specifically, Taylor et al.[22] constructed intracranial EEG normative maps using the spared electrodes of 234 focal epilepsy patients who later went on to have successful surgical outcomes (ILAE 1 and 2). We directly compare these normative maps in figure S1 and report strong spatial similarities in the delta, alpha and beta frequency bands. Weaker associations in the theta band could be attributed to alpha de-synchronisation, an effect commonly reported between eyes open and closed data recordings, with reductions in alpha power. The discrepancies in gamma spatial distributions across modalities are possibly due to the lower signal to noise ratio at higher frequencies.

During the pre-surgical evaluation, interictal MEG recordings are used clinically to identify and localise interictal spikes as markers of the epileptogenic zone. However, the origin and pathological nature of spikes has been questioned, with some studies suggesting a protective effect[50], and others suggesting their resection does not improve outcomes[51]. Given this ambiguity, and the high expense of MEG, their clinical use is less common during pre-surgical evaluation, and are typically reserved for patients with difficult to localise seizure foci. We leverage the usually discarded interictal data, demonstrating that even seemingly normal recordings can contain clinically valuable information for the localisation of epileptogenic tissue. Beyond application to traditional MEG data, as shown here, future studies could apply our markers of surgical failure to scalp EEG, or less expensive portable MEG[52].

Several limitations of this work should be noted. First, although a large cohort of controls were used, the patient sample size used in this study is relatively low. This in turn prevented us from predicting surgical outcome using traditional data-driven machine learning techniques in order to avoid the issue of overfitting the data. Instead, we proposed intuitive and hypothesis-driven mechanisms which should generalise across patient cohorts. As a result, our simultaneous analysis of surgical failure mechanisms resulted in 50% of seizure free patients exhibiting at least one marker of surgical failure. The large false negative rate is likely attributed to the univariate thresholds set to optimally separate surgical outcome groups. Future studies with larger sample sizes could use machine learning algorithms to optimally separate surgical outcome groups in

higher dimensions. Alternatively, clinical demographics and functional data could be harmonised into a single predictive models as has been previously done using structural abnormalities[15,17], minimising the large false negative rate reported in our study. A second limitation of this work is the poor signal to noise of resting state MEG for subcortical structures such as the hippocampus and amygdala, with challenges due to the inverse problem. This is particularly problematic for resting state low amplitude activity as studied here. Due to these factors, we excluded deep brain structures from our analysis, and include patients with hippocampal resections only as supplementary material. Finally, our normative data was acquired at a different site to that of our patients. However, both sites used a 275 CTF MEG scanner and a 3T GE Signa HDx scanner, which we expect mitigates site differences to a large extent. Additionally, our use of relative band power as a standardisation will also aid site normalization to some extent as in our previous work[22]. Furthermore, although our normative data is used as a baseline, the main statistical comparisons regarding surgical outcome are made between patients from the same site and are therefore unaffected by site differences.

Surgical resection of the epileptogenic zone is a treatment option for patients with refractory focal epilepsy. At present, it is not fully understood why surgical intervention in some patients is unsuccessful, though different reasons may explain for different patients. In this study we proposed three mechanisms which relate to surgical failure, demonstrating that they are robust to different epochs and parcellation schemes as shown in supplementary S1.3. These mechanisms, used in conjunction to clinical demographics could aid clinicians during the pre-surgical evaluation of patients. Future studies could derive additional mechanisms of surgical failure, with a focus on functional and structural networks, and combine all markers into a predictive model of surgical outcome.

Acknowledgements

References

1.   Stafstrom CE, Carmant L. Seizures and Epilepsy: An Overview for Neuroscientists. *Cold Spring Harbor Perspectives in Medicine*. 2015;5(6):a022426. doi:10.1101/cshperspect.a022426

2.   Tisi J de, Bell GS, Peacock JL, et al. The long-term outcome of adult epilepsy surgery, patterns of seizure remission, and relapse: A cohort study. *The Lancet*. 2011;378(9800):1388-1395. doi:10.1016/S0140-6736(11)60890-8

3.   Cohen-Gadol AA, Wilhelmi BG, Collignon F, et al. Long-term outcome of epilepsy surgery among 399 patients with nonlesional seizure foci including mesial temporal lobe sclerosis. *Journal of Neurosurgery*. 2006;104(4):513-524. doi:10.3171/jns.2006.104.4.513

4.   Englot DJ, Raygor KP, Molinaro AM, et al. Factors Associated With Failed Focal Neocortical Epilepsy Surgery. *Neurosurgery*. 2014;75(6):648-656. doi:10.1227/NEU.0000000000000530

5.   Bell GS, Tisi J de, Gonzalez-Fraile JC, et al. Factors affecting seizure outcome after epilepsy surgery: An observational series. *Journal of Neurology, Neurosurgery & Psychiatry*. 2017;88(11):933-940. doi:10.1136/jnnp-2017-316211

6.   Morgan VL, Rogers BP, González HFJ, Goodale SE, Englot DJ. Characterization of postsurgical functional connectivity changes in temporal lobe epilepsy. *Journal of neurosurgery*. Published online June 2019:1-11. doi:10.3171/2019.3.JNS19350

7.   Barba C, Rheims S, Minotti L, et al. Temporal plus epilepsy is a major determinant of temporal lobe surgery failures. *Brain*. 2016;139(2):444-451. doi:10.1093/brain/awv372

8.   Morgan VL, Sainburg LE, Johnson GW, et al. Presurgical temporal lobe epilepsy connectome fingerprint for seizure outcome prediction. *Brain Communications*. Published online May 2022:fcac128. doi:10.1093/braincomms/fcac128

9.   Bartolomei F, Lagarde S, Wendling F, et al. Defining epileptogenic networks: Contribution of SEEG and signal analysis. *Epilepsia*. 2017;58(7):1131-1147. doi:10.1111/epi.13791

10.   Assaf BA, Karkar KM, Laxer KD, et al. Magnetoencephalography source localization and surgical outcome in temporal lobe epilepsy. *Clinical Neurophysiology*. 2004;115(9):2066-2076. doi:10.1016/j.clinph.2004.04.020

11.   Englot DJ, Hinkley LB, Kort NS, et al. Global and regional functional connectivity maps of neural oscillations in focal epilepsy. *Brain*. 2015;138(8):2249-2262. doi:10.1093/brain/awv130

12.   Nissen IA, Stam CJ, Reijneveld JC, et al. Identifying the epileptogenic zone in interictal resting-state MEG source-space networks. *Epilepsia*. 2017;58(1):137-148. doi:10.1111/epi.13622

13.   Aydin Ü, Pellegrino G, Bin Ka'b Ali O, et al. Magnetoencephalography resting state connectivity patterns as indicatives of surgical outcome in epilepsy patients. *Journal of Neural Engineering*. Published online March 2020. doi:10.1088/1741-2552/ab8113

14.   Ramaraju S, Wang Y, Sinha N, et al. Removal of Interictal MEG-Derived Network Hubs Is Associated With Postoperative Seizure Freedom. *Frontiers in Neurology*. 2020;11. doi:10.3389/fneur.2020.563847

15.   Bonilha L, Jensen JH, Baker N, et al. The brain connectome as a personalized biomarker of seizure outcomes after temporal lobectomy. *Neurology*. 2015;84(18):1846-1853. doi:10.1212/WNL.0000000000001548

16.   Keller SS, Glenn GR, Weber B, et al. Preoperative automated fibre quantification predicts postoperative seizure outcome in temporal lobe epilepsy. *Brain*. 2017;140(1):68-82. doi:10.1093/brain/aww280

17.   Sinha N, Wang Y, Silva NM da, et al. *Node Abnormality Predicts Seizure Outcome and Relates to Long-Term Relapse After Epilepsy Surgery*. Neuroscience; 2019. doi:10.1101/747725

18.   Owen TW, Tisi J de, Vos SB, et al. Multivariate white matter alterations are associated with epilepsy duration. *European Journal of Neuroscience*. 2021;53(8):2788-2803. doi:10.1111/ejn.15055

19.   Frauscher B, Ellenrieder N von, Zelmann R, et al. Atlas of the normal intracranial electroencephalogram: Neurophysiological awake activity in different cortical areas. *Brain: A Journal of Neurology*. 2018;141(4):1130-1144. doi:10.1093/brain/awy035

20.   Bosch-Bayard J, Aubert-Vazquez E, Brown ST, et al. A Quantitative EEG Toolbox for the MNI Neuroinformatics Ecosystem: Normative SPM of EEG Source Spectra. *Frontiers in Neuroinformatics*. 2020;14. Accessed May 31, 2022. https://www.frontiersin.org/article/10.3389/fninf.2020.00033

21.   Kudo K, Morise H, Ranasinghe KG, et al. Magnetoencephalography Imaging Reveals Abnormal Information Flow in Temporal Lobe Epilepsy. *Brain Connectivity*. Published online July 2021. doi:10.1089/brain.2020.0989

22.   Taylor PN, Papasavvas CA, Owen TW, et al. Normative brain mapping of interictal intracranial EEG to localize epileptogenic tissue. *Brain*. Published online January 2022:awab380. doi:10.1093/brain/awab380

23.   Wieser HG, Blume WT, Fish D, et al. Proposal for a New Classification of Outcome with Respect to Epileptic Seizures Following Epilepsy Surgery. *Epilepsia*. 2001;42(2):282-286. doi:10.1046/j.1528-1157.2001.35100.x

24.   Taylor PN, Sinha N, Wang Y, et al. The impact of epilepsy surgery on the structural connectome and its relation to outcome. *NeuroImage: Clinical*. 2018;18:202-214. doi:10.1016/j.nicl.2018.01.028

25.   Messaritaki E, Foley S, Schiavi S, et al. Predicting MEG resting-state functional connectivity from microstructural information. *Network Neuroscience*. Published online April 2021:1-28. doi:10.1162/netn_a_00187

26.   Fischl B. FreeSurfer. *NeuroImage*. 2012;62(2):774-781. doi:10.1016/j.neuroimage.2012.01.021

27.   Hagmann P, Cammoun L, Gigandet X, et al. Mapping the Structural Core of Human Cerebral Cortex. *PLOS Biology*. 2008;6(7):e159. doi:10.1371/journal.pbio.0060159

28.   Jenkinson M, Smith S. A global optimisation method for robust affine registration of brain images. *Medical Image Analysis*. 2001;5(2):143-156. doi:10.1016/S1361-8415(01)00036-6

29.   Jenkinson M, Bannister P, Brady M, Smith S. Improved Optimization for the Robust and Accurate Linear Registration and Motion Correction of Brain Images. *NeuroImage*. 2002;17(2):825-841. doi:10.1006/nimg.2002.1132

30.   Greve DN, Fischl B. Accurate and robust brain image alignment using boundary-based registration. *NeuroImage*. 2009;48(1):63-72. doi:10.1016/j.neuroimage.2009.06.060

31.   Tadel F, Baillet S, Mosher JC, Pantazis D, Leahy RM. Brainstorm: A user-friendly application for MEG/EEG analysis. *Computational Intelligence and Neuroscience*. 2011;2011:879716. doi:10.1155/2011/879716

32.   Wang Y, Sinha N, Schroeder GM, et al. Interictal intracranial electroencephalography for predicting surgical success: The importance of space and time. *Epilepsia*. 2020;61(7):1417-1426. doi:10.1111/epi.16580

33.   Jehi L, Yardi R, Chagin K, et al. Development and validation of nomograms to provide individualised predictions of seizure outcomes after epilepsy surgery: A retrospective analysis. *The Lancet Neurology*. 2015;14(3):283-290. doi:10.1016/S1474-4422(14)70325-4

34.   Scholtens LH, Lange SC de, Heuvel MP van den. Simple brain plot. Published online August 2021. doi:10.5281/zenodo.5346593

35.   Bernabei JM, Arnold TC, Shah P, et al. Electrocorticography and stereo EEG provide distinct measures of brain connectivity: Implications for network models. *Brain Communications*. 2021;3(3):fcab156. doi:10.1093/braincomms/fcab156

36.   Kim DW, Lee SK, Moon HJ, Jung KY, Chu K, Chung CK. Surgical Treatment of Nonlesional Neocortical Epilepsy: Long-term Longitudinal Study. *JAMA Neurology*. 2017;74(3):324-331. doi:10.1001/jamaneurol.2016.4439

37.   Tsuda K, Tsuji T, Ishida T, et al. Widespread abnormalities in white matter integrity and their relationship with duration of illness in temporal lobe epilepsy. *Epilepsia Open*. 2018;3(2):247-254. doi:10.1002/epi4.12222

38.   Hatton SN, Huynh KH, Bonilha L, et al. White matter abnormalities across different epilepsy syndromes in adults: An ENIGMA Epilepsy study. *bioRxiv*. Published online December 2019:2019.12.19.883405. doi:https://doi.org/10.1101/2019.12.19.883405

39.   Gupta K, Grover P, Abel TJ. Current Conceptual Understanding of the Epileptogenic Network From Stereoelectroencephalography-Based Connectivity Inferences. *Frontiers in Neurology*. 2020;11. Accessed July 1, 2022. https://www.frontiersin.org/article/10.3389/fneur.2020.569699

40.   Worsley KJ, Taylor JE, Carbonell F, et al. SurfStat: A Matlab toolbox for the statistical analysis of univariate and multivariate surface and volumetric data using linear mixed effects models and random field theory. *Neuroimage*. Published online July 2009. doi:10.1016/S1053-8119(09)70882-1

41.   Rey SJ, Smith RJ. A spatial decomposition of the Gini coefficient. *Letters in Spatial and Resource Sciences*. 2013;6(2):55-70. doi:10.1007/s12076-012-0086-z

42.   Silva NM da, Forsyth R, McEvoy A, et al. Network reorganisation following anterior temporal lobe resection and relation with post-surgery seizure relapse: A longitudinal study. *NeuroImage: Clinical*. 2020;27:102320. doi:10.1016/j.nicl.2020.102320

43.   Delorme A, Palmer J, Onton J, Oostenveld R, Makeig S. Independent EEG Sources Are Dipolar. Ward LM, ed. *PLoS ONE*. 2012;7(2):e30135. doi:10.1371/journal.pone.0030135

44.   Hillebrand A, Barnes GR, Bosboom JL, Berendse HW, Stam CJ. Frequency-dependent functional connectivity within resting-state networks: An atlas-based MEG beamformer solution. *Neuroimage*. 2012;59(4-2):3909-3921. doi:10.1016/j.neuroimage.2011.11.005

45.   Gómez C, Pérez-Macías JM, Poza J, Fernández A, Hornero R. Spectral changes in spontaneous MEG activity across the lifespan. *Journal of Neural Engineering*. 2013;10(6):066006. doi:10.1088/1741-2560/10/6/066006

46.   Niso G, Rogers C, Moreau JT, et al. OMEGA: The Open MEG Archive. *NeuroImage*. 2016;124:1182-1187. doi:10.1016/j.neuroimage.2015.04.028

47.   Gómez CM, Rodríguez-Martínez EI, Fernández A, Maestú F, Poza J, Gómez C. Absolute Power Spectral Density Changes in the Magnetoencephalographic Activity During the Transition from Childhood to Adulthood. *Brain Topography*. 2017;30(1):87-97. doi:10.1007/s10548-016-0532-0

48.   Niso G, Tadel F, Bock E, Cousineau M, Santos A, Baillet S. Brainstorm Pipeline Analysis of Resting-State Data From the Open MEG Archive. *Frontiers in Neuroscience*. 2019;13. doi:10.3389/fnins.2019.00284

49.   Markello RD, Hansen JY, Liu ZQ, et al. *Neuromaps: Structural and Functional Interpretation of Brain Maps*.; 2022:2022.01.06.475081. doi:10.1101/2022.01.06.475081

50.   Avoli M, Biagini G, Curtis M de. Do Interictal Spikes Sustain Seizures and Epileptogenesis? *Epilepsy Currents*. 2006;6(6):203-207. doi:10.1111/j.1535-7511.2006.00146.x

51.   Rosenow F, Lüders H. Presurgical evaluation of epilepsy. *Brain*. 2001;124(9):1683-1700. doi:10.1093/brain/124.9.1683

52.   Boto E, Holmes N, Leggett J, et al. Moving magnetoencephalography towards real-world applications with a wearable system. *Nature*. 2018;555(7698):657-661. doi:10.1038/nature26147

53.   Barry RJ, Clarke AR, Johnstone SJ, Magee CA, Rushby JA. EEG differences between eyes-closed and eyes-open resting conditions. *Clinical Neurophysiology*. 2007;118(12):2765-2773. doi:10.1016/j.clinph.2007.07.028

54.   Barry RJ, De Blasio FM. EEG differences between eyes-closed and eyes-open resting remain in healthy ageing. *Biological Psychology*. 2017;129:293-304. doi:10.1016/j.biopsycho.2017.09.010